ZEBRAFISH
Volume 7, Number 4, 2010

DOI: 10.1089/zeb.2010.0663

Enforced Expression of Simian Virus 40 Large T-Antigen Leads to Testicular Germ Cell Tumors in Zebrafish

James A. Gill,[1] Linda Lowe,[1] Joan Nguyen,[1] P. Paul Liu,[2] Trevor Blake,[2]
Byrappa Venkatesh,[3] and Peter D. Aplan[1]

Abstract

Testicular germ cell tumors (TGCTs) are the most common malignancy in young men. However, there are few *in vivo* animal models that have been developed to study this disease. We have used the pufferfish (fugu) lymphocyte-specific protein tyrosine kinase (*flck*) promoter, which has been shown to enforce high-level expression in the testes of transgenic mice, to express Simian virus 40 large T-antigen in zebrafish testes. Zebrafish that express T-antigen develop TGCTs after a long latency of >1 year. Although overt TGCTs are only evident in 20% of the fish, occult TGCTs can be detected in 90% of the transgenic fish by 36 month of age. The TGCTs resemble the human disease in terms of morphology and gene expression pattern, and can be transplanted to healthy wild-type recipient fish. In addition, enforced expression of the zebrafish stem cell leukemia (*scl*) gene in the zebrafish testes also generated TGCTs in transgenic fish. These results demonstrate the feasibility of studying TGCTs in a model organism.

Introduction

Testicular germ cell tumors (TGCTs) comprise up to 60% of all malignancies in men between 20 and 40 years of age.[1] Half of all diagnosed TGCTs are seminomas, 30% are nonseminomas, and the remaining combine both seminoma and nonseminoma components. The more aggressive nonseminomas manifest at a younger age (median age at diagnosis 25 years) than seminomas, which appear in older patients (median age at diagnosis 35 years). This may be due to a loss in older populations of the original germ-cell's stem-cell capacity.[2] While seminomas are chemo- and radiosensitive, patients with nonseminoma TGCTs have cure rates dependent of disease stage, some as low as 50%.[3] At the time of diagnosis a significant percentage of TGCTs are metastatic, and 10%–20% of patients with metastatic TGCTs fail to achieve complete remission,[4] thus providing incentives for improvements in diagnosis. Additionally, the endogenous or environmental factors affecting the origins of TGCTs are poorly understood.

The zebrafish is an attractive vertebrate model due to its high fecundity, genetic accessibility, and embryonic transparency. Additionally, evidence suggests that teleost gonadal development is less strictly genetic than in mammals, being partially governed by secondary environmental effects, and the resulting developmental plasticity may facilitate investigation into the environmental factors affecting TGCTs. Interest in modeling TGCTs in zebrafish has lead to the recent identification of a mutant zebrafish line that develops TGCTs through a large-scale forward genetics screen.[5] Sex determination and gonadal differentiation in zebrafish has not been fully elucidated; however, conserved and divergent functions in gonadal development, compared to the well-understood mammalian system, have been proposed.[6,7] For instance, there is little evidence suggesting that zebrafish have sex chromosomes, and though the developmental stage at which sex determination occurs is unknown, there is a latency period in testis development during which males undergo a "compulsory ovary stage."[7] Conversely, sexually mature teleost and mammal gonads both contain Sertoli and Leydig cells, as well as germ cells. Similar to humans, male zebrafish seminiferous tubules are composed of compartmentalized spermatogonia, spermatocytes, and tail-less spermatids, suggesting similar developmental pathways.

In this study, we report two zebrafish models for TGCT. These zebrafish models can be used for large-scale genetic modifier screens to elucidate mutant genes related to the malignant phenotype. As zebrafish are amenable to studying the environmental factors in disease pathology, these models may be beneficial for elucidating the endogenous and environmental component of TGCTs.

[1]Genetics Branch, Center for Cancer Research, National Cancer Institute and [2]Genetics and Molecular Biology Branch, National Human Genome Research Institute, NIH, Bethesda, Maryland.
[3]Institute of Molecular and Cell Biology, A*STAR, Biopolis, Singapore.

Methods

Vectors

Simian virus 40 (SV40) T-antigen (*TAg*), stem cell leukemia (*scl*), and lim domain only 1 (*lmo1*) transgenes were polymerase chain reaction (PCR) amplified and cloned into a 4.2-kb F3R1-11 backbone, which contains both the proximal and distal fugu lymphocyte-specific protein tyrosine kinase (*lck*) promoter regions controlling expression of green fluorescent protein (EGFP).[8] The EGFP cDNA was replaced by the indicated cDNA (*TAg*, *scl*, or *lmo1*). Inserts containing both the proximal and distal fugu *lck* promoters and the indicated cDNA sequence were isolated and purified (Qiagen). The F3R1-11 plasmid was digested with *Xho*I and *Sfi*I, the *flck:lmo1* plasmid was digested with *Sfi*I and *Bgl*II, and both the *flck:TAg* and *flck:scl* plasmids were digested with *Bgl*II and *Not*I (Fig. 1A).

Zebrafish maintenance

To generate *Tg(flck:TAg)*, *Tg(flck:scl)*, and *Tg(flck:lmo1)* transgenic fish, an AB/TU line was used (originally obtained from Dr. Brant Weinstein, NIH/NICHD). Fish were housed in an automatic fish housing systems (Aquatic Habitats) at 28.5°C. All zebrafish manipulations were approved by the NCI Animal Care and Use Committee.

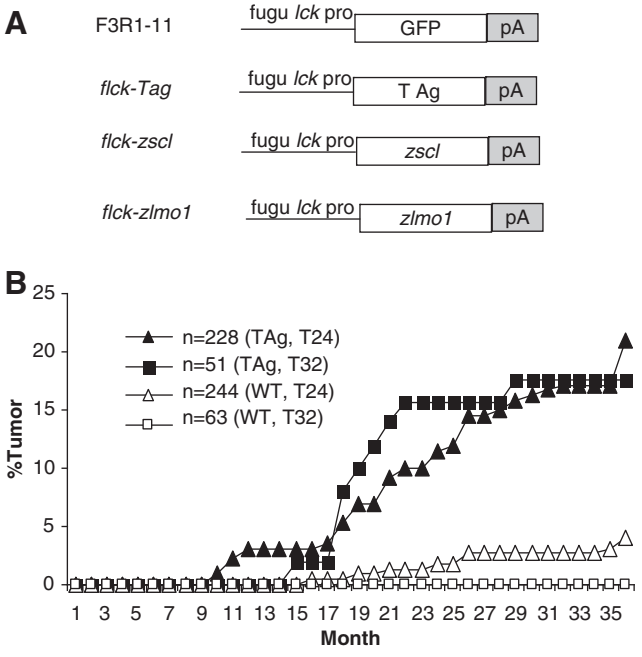

FIG. 1. Abdominal tumor development in *Tg(flck:TAg)* fish. **(A)** Vectors used to generate transgenic zebrafish. pro, promoter region; pA, Simian virus 40 polyadenylation signal. **(B)** Cumulative abdominal tumor frequency in two independent transgenic lines expressing TAg (T24 and T32), compared to nontransgenic WT fish from the same clutch. Log rank *p*-value for T24 transgenic versus WT = 0.0198; for T32 transgenic vs. WT = 0.0005. The number of fish in each series is indicated. TAg, T-antigen; WT, wild-type.

Generation of transgenic fish

To generate transgenic fish, freshly laid AB/TU eggs were injected with purified DNA fragments. The purified fragments were resuspended at a final concentration of 50 ng/μL in 0.5% Phenol Red. One hundred picograms of insert was injected into zebrafish embryos at the one-cell stage with a PV820 Pneumatic PicoPump (World Precision Instruments, Inc.). For a typical experiment, 50–100 fertilized eggs would be injected, within ~45 min, before the first cell division. Approximately half of the injected eggs survived to produce adult fish. Positive mosaic F0 fish were identified by PCR amplification of fin clip DNA; primers used are listed in Supplementary Table S1 (Supplementary Data are available online at www.liebertonline.com/zeb). None of the primers used for genotyping generated an amplification product in wild-type (WT) fish, and amplification of a cellular retinoic acid-binding protein (*crab*) gene fragment was used to assess genomic DNA quality. The positive mosaic F0 fish were then bred to AB/TU WT fish to determine if they could transmit the transgene. Typically, 10%–40% of the positive, mosaic adult fish were able to transmit the transgene and become founders. Stable lines of transgenic fish were obtained from *Tg(flck:TAg)*, *Tg(flck:scl)*, and *Tg(flck:lmo1)* F0 founder fish and maintained by backcrossing to AB/TU WT fish.

Tumor cell analysis

Before tissue collection, zebrafish were euthanized by adding 0.3 g tricaine to 0.8 g NaCl and dissolving in 1 L of system water. Tumor tissue was extracted following a ventral, sagittal incision and either fixed in neutral buffered 10% formalin solution for histological preparation, placed into ice-cold 0.9×phosphate-buffered saline containing 5% fetal bovine serum for single-cell suspension, or frozen for nucleic acid isolation. Parafin embedding, sectioning, and staining was performed by HistoServ, Inc. Photomicrographs were taken with a Fuji FinePix 6800Z camera (Fuji) with a Carl Zeiss Standard 25 ICS microscope and a custom eyepiece adaptor (Accuscope). All original magnifications were between 50 and 1000×. *In vivo* imaging of EGFP fluorescence was observed with a Leica ebq 100 mercury vapor lamp and Carl Zeiss Stemi SV11 dissecting microscope.

Flow cytometry

Harvested tissue from transgenic fish was dissociated by glass pestle in ice-cold 0.9× phosphate-buffered saline. To facilitate single-cell suspension, tissue was incubated at 22°C for 45 min in 5 mL of 4 μg collagenase per mL of HBSS, and strained through a 40-micron nylon mesh filter.[9] Cells were centrifuged at 1000× *g* and resuspended in ice-cold Hanks' balanced salt solution with 2% fetal bovine serum. Propidium iodide (Sigma) was added at 1 μg/mL to exclude dead cells and debris. FACS analysis and sorting were performed based on propidium iodide exclusion, forward scatter, and side scatter using a FACScan (Becton Dickinson).

Tumor cell transplantation

Cell suspensions were prepared from moribund transgenic *Tg(flck:TAg)* fish as described above. About 5×10^3 cells were injected intraperitoneally into 12-month-old WT male

recipients using a 30½-gauge PrecisionGlide needle, after anesthesia with tricaine.

Southern blots for T-cell receptor alpha configuration

Zebrafish-specific primers were used to generate a probe for the C region of T-cell receptor alpha (*tcra*) (accession No. AF246178).[8] Genomic DNA from tumor and control tissue was digested with *Hin*dIII, *Bgl*II, or *Eco*RI; size fractioned on 0.8% agarose gels; denatured; transferred to nitrocellulose membranes; and hybridized to a 32P probe, labeled by random priming, as previously described.[9]

Reverse transcription-PCR analysis

Total RNA was isolated using TRIZOL (Invitrogen) reagent and the manufacturer's recommended protocol. About 1.0 μg of total RNA from each extraction was reverse-transcribed and PCR was carried out. Primers used are indicated in supplementary Table S1.

Results

Generation of transgenic zebrafish

Our initial goal was to generate thymic tumors in zebrafish, to allow comparative genomics to highlight conserved pathways among human, mouse, and zebrafish T-cell malignancies. In an effort to generate thymic malignancies in zebrafish, we generated transgenic fish that expressed either *SV40* large *TAg*, zebrafish *scl* (*scl*), or zebrafish *lmo1* in the thymus of the developing zebrafish. All of these genes (except *TAg*) are associated with thymic malignancies in humans and have been demonstrated to produce thymic malignancies when overexpressed in the mouse thymus.[9,10] We used *lck* regulatory elements from fugu, which have been reported to be functional in fugu thymocytes,[11] because *lck* regulatory elements have been used previously to express transgenes in the mouse and zebrafish thymus (Fig. 1A).[12,13]

Tg(flck:TAg), *Tg(flck:scl)*, and *Tg(flck:lmo1)* transgenic fish were generated by microinjection of DNA into one-cell stage zebrafish embryos. Mosaic F0 transgenic fish were identified by PCR genotyping of fin biopsies. Two selected mosaic F0 fish were then bred to WT fish, and transmission of the transgene was identified by genotyping the F1 offspring. Although the fish embryos were injected at the one-cell stage, due to rapid cell division, the transgene may not integrate into genomic DNA until the two-cell stage or later. Therefore, the founder fish are likely to be mosaic for the transgene, and the germ cells may not be transgenic. One hundred seventy-four embryos injected with the *flck:TAg* vector (Fig. 1A) survived to adulthood, 12 of which were mosaic. Three of these were transgenic in their germ cells for the *flck:TAg* vector and transmitted the transgene, as determined by genotyping fins of F1 offspring, or genotyping pooled F1 embryos. The three *Tg(flck:TAg)* founder lines were designated T9, T24, and T32. To avoid the possibility of integration effects, we chose to focus our studies on two independent *Tg(flck:TAg)* lines derived from separate injections (T24 and T32).

Tg(flck:TAg) *fish develop abdominal tumors*

A survival cohort of transgenic fish was observed for 36 months. At 11 months, some of the *Tg(flck:TAg)* transgenic males developed visible abdominal enlargement, but exhibited no other obvious signs of disease. Affected fish had asymmetric enlargement of the abdomen rather than the symmetrical enlargement typically seen in other disorders such as egg binding and *Mycobacteria* sp. infections.[14,15] Abdominal skin overlying the tumors was thinned and showed vascular congestion. Internally, the tumors filled the abdomen and caused pressure atrophy of surrounding intra-abdominal organs.

Given the use of the *flck* promoter, which we had shown to be functional in the zebrafish thymus, the tumors were initially suspected to be of thymic origin, with metastasis to the testes. Hematoxylin and eosin histology on some tumors resembled T-lymphoblasts (see below), with sheets of small basophilic cells and a high nuclear/cytoplasmic ratio invading the testes. However, we never detected thymic enlargement in these fish, and some tumors had marked overgrowth of spermatogonial-like cells, calling into question the diagnosis of thymic tumors. To further investigate the possibility of a thymic malignancy, we looked for evidence of clonal T-cell receptor gene rearrangement in tumor samples. However, the tumor DNA showed no evidence of clonal *tcra* gene rearrangement (Supplementary Fig. S1), making the diagnosis of thymic tumors unlikely. Subsequently, additional fish (between 16% and 20% of the transgenic offspring) from both the T24 and T32 founders developed abdominal tumors (Fig. 1B). In addition, the T9 founder also developed an abdominal tumor. In contrast, <4% of the WT nontransgenic control fish from this cohort developed abdominal tumors over the 3-year study period. The observation that abdominal tumors occurred in three independent *Tg(Tg(flck:TAg))* transgenic lines indicated that tumor predisposition was not due to an unexpected integration effect of the transgenic vector.

Initially, fish with obvious abdominal swelling were observed closely, and showed normal swimming ability and patterns. Despite this close observation, occasional fish with abdominal swelling were found dead, indicating that the abdominal tumors were progressive and lethal. With the assistance of aquatic caretakers we gained more experience, and fish with abdominal tumors were euthanized and only rarely found dead.

The abdominal tumors are TGCTs

The abdominal tumors were clearly evident to the naked eye; an example is shown in Figure 2A. Upon gross inspection, the tumors were firm, white or tan in color, and nodular, ranging in size from 4 to 8 mm in diameter at their widest point. Histological analysis suggested that these tumors were not of thymic origin, but were instead TGCTs. A gross comparison of a fish TGCT and WT fish testes is shown in Figure 2.

Three prominent cell populations are recognized in normal zebrafish testis: spermatogonia, spermatocytes, and spermatids (Fig. 2D). Zebrafish spermatogonia are between 7 and 9 μm in diameter with a relatively low nuclear-to-cytoplasm ratio. Spermatocytes are slightly smaller with a high nuclear-to-cytoplasm ratio, and spermatids are fairly uniform in size, typically 2 μm in diameter, and are the smallest and densest of these three cell types. Although the normal fish testis is arranged into seminiferous tubules composed of well-organized spermatogonial cells, with spermatocytes and spermatids located in the lumen, the fish TGCT lack these

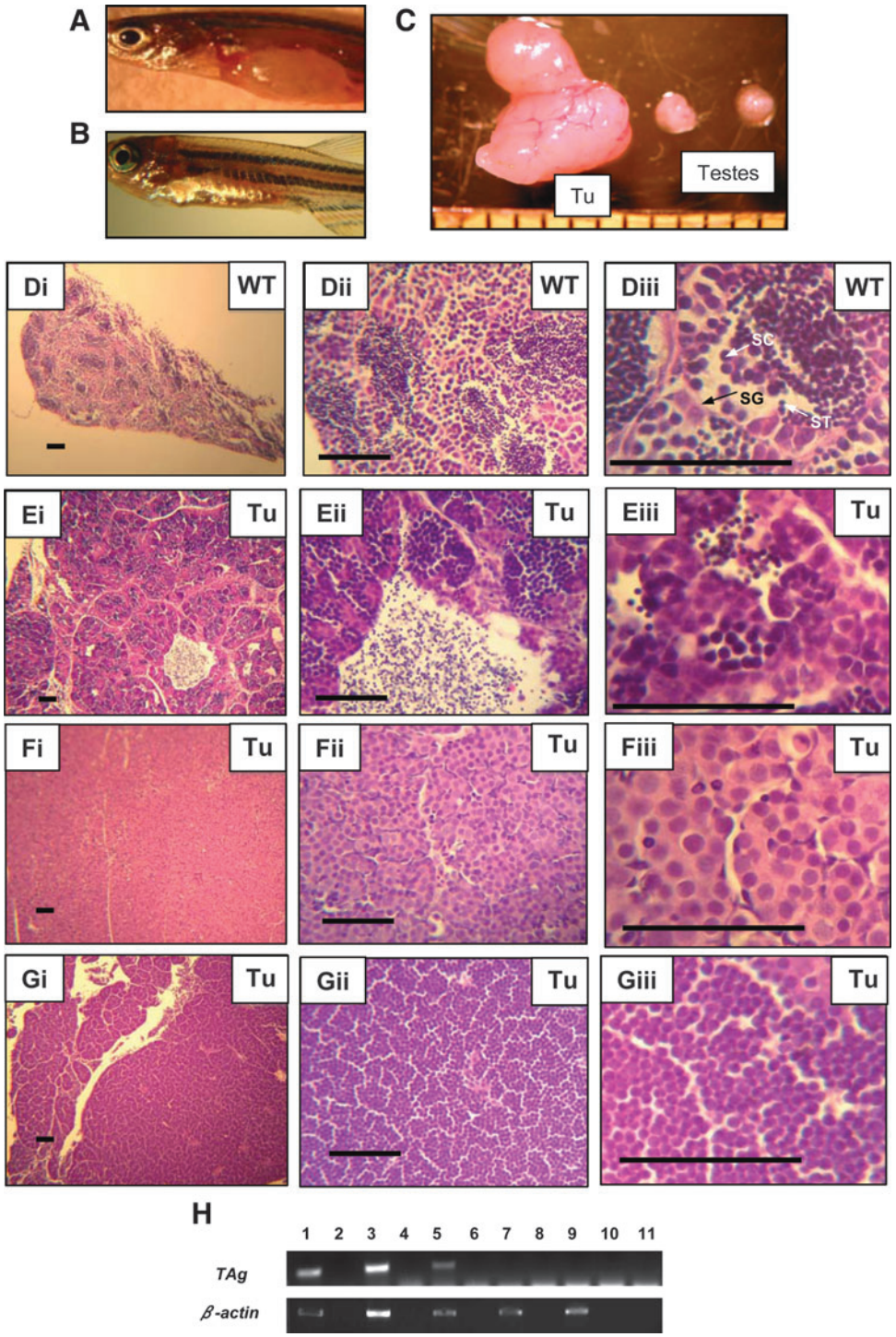

FIG. 2. Characterization of abdominal tumors. **(A)** Gross photo of *flck:TAg* zebrafish with abdominal tumor. **(B)** WT male zebrafish for comparison **(C)** testicular germ cell tumor (Tu) compared to WT testes. Size scale is in mm. **(Di–Diii**) Hematoxylin and eosin-stained testis from WT fish at low, medium, and high power, respectively. Scale bar is 50 μm in all photos. Spermatogonia (SG), spermatocytes (SC), and spermatids (ST) are indicated in **(Diii)**. **(Ei–Eiii)** TGCT from *flck:TAg* fish T32(25), same magnifications as above. Note wide spectrum of different cell sizes and morphology. **(Fi–Fiii)** TGCT from *flck:TAg* fish T24 (10), same magnifications as above. Note the uniform population of cells with abundant eosinophilic cytoplasm and a low nuclear-to-cytoplasmic ratio, consistent with spermatogonial cells. **(Gi–Giii)** TGCT from *flck:TAg fish* T24(4), same magnifications as above. Note the uniform population of basophilic cells with a high nuclear-to-cytoplasmic ratio, consistent with spermatocytes. **(H)** Reverse transcription-polymerase chain reaction assay for TAg expression. Lanes 1–4, TGCT from two independent *Tg(flck:TAg)* fish; lanes 5 and 6, testes from a clinically healthy *Tg(flck:TAg)* fish without TGCT; lanes 7 and 8, WT testes; lanes 9 and 10, gill from clinically healthy *Tg(flck:TAg)* fish; lane 11, dH_2O. Reverse transcriptase was not added to the cDNA reactions in lanes 2, 4, 6, 8, and 10. Polymerase chain reaction amplification for TAg or β-actin is shown. TGCTs, testicular germ cell tumors.

organized structures. Figure 2E–G shows a spectrum of histology identified in the fish TGCTs. Figure 2E shows a TGCT composed of a heterogeneous population of cells that resemble spermatocytes and spermatogonial cells, whereas Figure panels 2F and 2G show TGCTs predominantly composed of monotonous sheets of cells that resemble either spermatogonia or spermatocytes, respectively. The lack of normal testicular architecture in seminiferous tubules, along with a variable, increased population of undifferentiated spermatogonial-like cells and/or spermatocytes, and deficiency of spermatids, supports the classification of these tumors as germ cell tumors of the testes.

Given that *LCK* expression has typically been considered to be restricted to lymphocytes, we analyzed the fish TGCT for evidence of *TAg* expression. As shown in Figure 2H, *TAg* mRNA is detected in transgenic testes and TGCTs, but not in WT testes or other transgenic tissues, such as gill. These findings are consistent with a prior report that demonstrated high level expression of *EGFP* in mouse testes driven by the 4.2 kb *flck* promoter fragment present on the F3-R1-11 plasmid backbone.[10]

Molecular analysis

To verify the testicular origin of these tumors, we assessed expression of a set of genes (*amh*, *wt1*, *cypllb*, *shippo1*, *sycp3l*, and *star*) that have been shown to be expressed in zebrafish testis. A zebrafish ortholog of the anti-Mullerian hormone (*amh*) gene and Wilm's tumor suppressor (*wt1*) gene have both been shown to be expressed in zebrafish Sertoli cells after differentiation, whereas *cytochrome p450* (*cyp11b*), a predominant androgen producing gene in zebrafish, is reported to be expressed primarily in Leydig cells in and around large clusters of spermatocytes.[16,17] The outer dense fiber of sperm tails (*Shippo1*) gene was identified as a spermatid marker in teleosts,[18,19] synaptonemal complex protein 3 like (*sycp3l*) is reported to be restricted to meiotic cells, and the steroidogenic acute regulatory (*star*) gene is expressed in zebrafish spermatogonial cells.[20]

In addition, we analyzed expression of several genes that have been reported to be differentially expressed between healthy human testes and seminomas; these included v-kit Hardy-Zuckerman 4 feline sarcoma viral oncogene (*kit*), progression of meiosis (*prom1*), POU domain, class 5, transcription factor 1 (*oct-4*), activating enhancer binding protein 2 alpha (*ap2α*), zinc finger and BTB domain containing 16 (*plzf*), and multiple coagulation factor deficiency 2 (*mcfd2*).[21–23] All the markers tested were expressed in *Tg(flck:TAg)* zebrafish TGCTs (Fig. 3), consistent with a testicular origin of these tumors. However, all the genes in this set were also detected in healthy zebrafish testes, indicating that these genes did not discriminate between clinically healthy testes and TGCTs in our zebrafish model (Fig. 3).

Since Kirsten, Harvey, and Neuroblastoma rat sarcoma viral oncogene (*KRAS*, *NRAS*, and *HRAS*) point mutations at codons 12, 13, and 61 are common in human patients with TGCTs,[24] we searched for *kras*, *nras*, and *hras* mutations in fish TGCTs. After establishing that these three genes were expressed in TGCT tissue (Supplementary Fig. S2) we sequenced genomic DNA from 10 *Tg(flck:TAg)* transgenic tumor samples across exons 1 and 2 in the zebrafish *kras*, *nras* and *hras* genes, and compared the sequences to those obtained from healthy nontransgenic, WT testis tissue (data not shown). There were no *de novo* mutations detected in codons 12, 13 and 61, or surrounding regions for *kras*, *nras*, or *hras*.

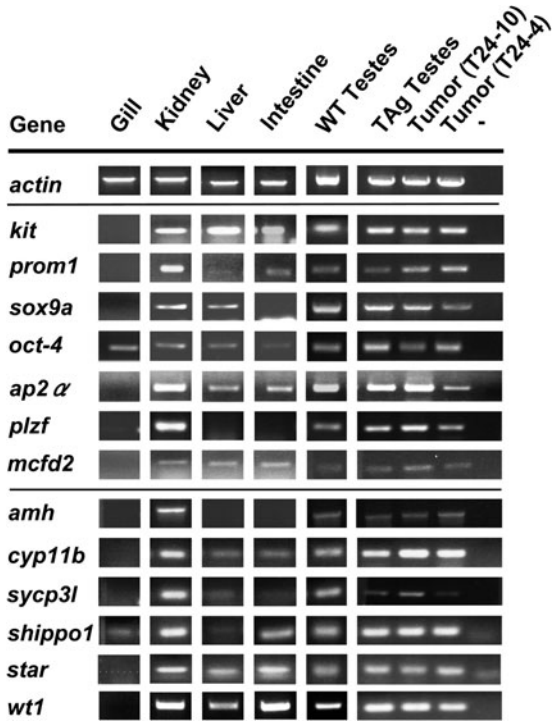

FIG. 3. Expression of TGCT markers: actin amplification is shown as an mRNA amplification control. Expression of *kit*, *prom1*, *sox9a*, *oct-4*, *ap2α*, *plzf*, *mcfd2*, *amh*, *cyp11b*, *sycp31*, *shippo1*, *star*, and *wt1* in transgenic gill, kidney, liver, intestine, testes, or WT testes are compared to two *Tg(flck:TAg)* TGCT samples [T24 (10) and T24 (4)]; (−) = dH_2O control.

The TGCTs are transplantable to WT fish

We further evaluated the malignancy of the tumors through transplant studies. A single-cell suspension of TGCT cells from *Tg(flck:TAg)* (line T24) donor fish or WT healthy testes was prepared, and 5×10^3 cells were injected into healthy 12-month-old WT, immunocompetent, syngeneic zebrafish. The recipient fish were monitored for 3 months postinjection. Two out of 50 recipients from the *Tg(flck:TAg)* TGCT donor developed tumors at 4 weeks postinjection. PCR analysis of genomic DNA from the recipient tumors demonstrated the presence of the *flck:TAg* transgene, using a *flck:TAg* primer set that does not amplify a product from the control zebrafish genome (data not shown), indicating that the tumor was derived from donor cells (Supplementary Fig. S3). There was no detectable tumor development in all 47 of the control group of fish injected with WT healthy testes.

Subclinical TGCTs

Because of the delayed onset of clinically evident TGCTs in our cohort, and the low but significant incidence of naturally occurring TGCTs in older WT male fish,[25,26] we wanted to determine the incidence of subclinical tumors in clinically healthy *Tg(flck:TAg)* transgenic fish. As an end-of-study experiment we euthanized clinically healthy WT and

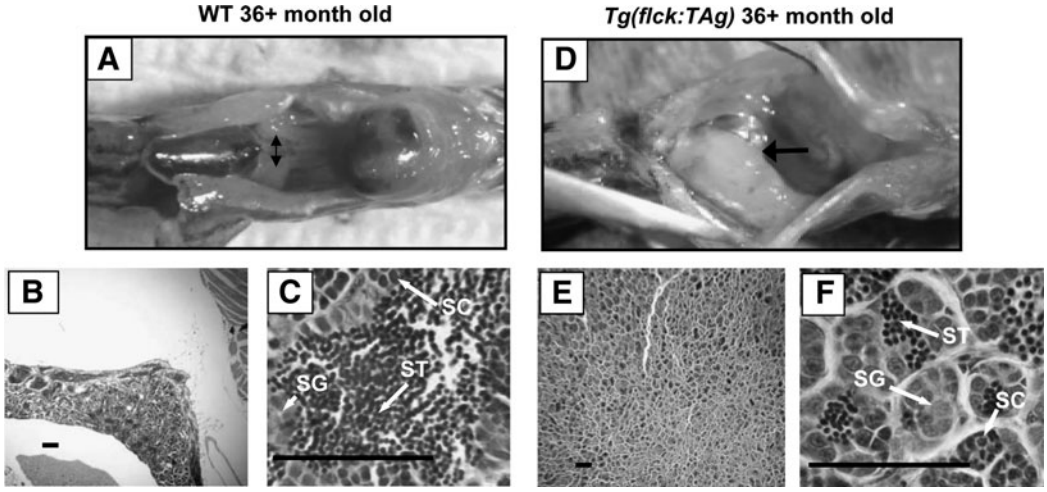

FIG. 4. Subclinical TGCT in *Tg(flck:TAg)* fish. **(A)** Representative non-TGCT testes in aged WT zebrafish. Arrows designate 2 separate, nonfused testes. **(B)** Aged non-TGCT zebrafish testis at low power (scale bar: 100 μm) **(C)** Aged non-TGCT zebrafish testis at high power (scale bar: 50 μm). **(D)** Subclinical TGCT in aged *Tg(flck:TAg)* zebrafish. Arrow indicates large, fused testes. **(E)** Aged sub-clinical TGCT at low power (scale bar: 100 μm). **(F)** Aged sub-clinical TGCT at high power (scale bar: 50 μm). Spermatogonia (SG), spermatocytes (SC), and spermatids (ST) are indicated in **(C)** and **(F)**.

Tg(flck:TAg) transgenic males that were over 36 months of age, with no evidence of abdominal masses (Fig. 4). We used two criteria for the diagnosis of a subclinical TGCT: testes fusion and enlargement of testicular tissue. Fifteen out of 30 (50%) clinically healthy WT aged male fish used in the experiment showed fused and enlarged testes (data not shown). However, 27 out of 30 (90%) *Tg(flck:TAg)* aged male fish had fused and enlarged testes (Fig. 4D–F). A previous study reported a tumor incidence of 48% in 29 WT male fish aged 30–34 months. These tumors were described as visibly large, noninvasive, and histologically composed of the range of cells common in spermatogenesis.[27] Figure 4A and 4D show the contrast between the distinct, small, bilateral testis in an aged WT fish, and an enlarged, fused testes in an aged *Tg(flck:TAg)* fish. Again, the histology of the subclinical TGCT was distinct from that of normal testes; the subclinical TGCT shown in Figure 4D–F is composed predominantly of spermatogonial-like cells, with a marked decrease in the number of spermatids (compare Fig. 4C and 4F).

TGCT in Tg(flck:scl) *and compound* Tg(flck:scl)/Tg(flck:lmo1) *fish*

In an additional effort to produce transgenic fish that developed T-cell acute lymphoblastic leukemia, we generated transgenic fish that expressed *scl* or *lmo1*, again under the control of the fugu *lck* promoter. After injection of the *flck:scl* construct, 165 injected eggs survived to adulthood and resulted in 4 of 12 mosaic fish expressing *Tg(flck:scl)* in their germline. Similar to the *Tg(flck:TAg)* fish, the *Tg(flck:scl)* fish developed TGCTs. As shown in Figure 5A, two independent lines of *Tg(flck:scl)* fish (designated U2 and Q1) developed TGCTs, with a time course similar to that of the *Tg(flck:TAg)* fish. Histologically, these tumors were similar to the *Tg(flck:TAg)* TGCTs (data not shown). However, we did not detect any evidence of T-cell malignancies in either line of *Tg(flck:scl)*fish. As expected, we detected expression of *scl* in the TGCT and transgenic testes, but not in WT testis or transgenic gill tissue (Fig. 5C).

In mice, Scl and Lmo1 collaborate to generate T-cell malignancies. To determine if these two genes would collaborate to generate T-cell malignancies in fish, we injected the *flck:lmo1* construct into fertilized eggs. Three hundred and eighty-two fish survived to adulthood, and from 12 positive mosaic fish there was a single founder. The resulting *Tg(flck:lmo1)* transgenic line was crossed to *Tg(flck:scl)* fish to produce *Tg(flck:scl)/Tg(flck:lmo1)* compound transgenic fish. Once again, these fish developed TGCTs, with a time course and histology similar to that of the *Tg(flck:TAg)* fish (Fig. 5B), but did not develop T-cell malignancies.

FACS analysis

To better characterize and quantify the sizes of cells present in a spectrum of fish TGCTs, from both the *Tg(flck:scl)* and the *Tg(flck:TAg)* lines, we used FACS analysis of transgenic tumor tissue and WT testes isolated from zebrafish adult males. FACS beads (SPHERO Calibration Particles, 6.0–6.4 μm) were used as a size standard for zebrafish testicular cell populations (Fig. 6). With a size standard we were able to divide a simple scatter plot into 2 μm increments and plot WT healthy testes and three samples of cells from transgenic TGCTs according to forward scatter. Since we wanted to compare a variety of histologically distinct TGCTs, resembling those previously shown in Figure 2, as well as compare TGCTs from both the *Tg(flck:scl)* and *Tg(flck:TAg)* lines, TGCTs from one of the *Tg(flck:scl)* lines and two of the *Tg(flck:TAg)* lines (U2, T24, and T32 respectively) were used. The FACS parameters were standardized across all the samples. The histology for WT testes, a *Tg(flck:scl)* TGCT from fish U2-6, and two *Tg(flck:TAg)* TGCTs from fish T32-8 and T24-14-6 (Fig. 6A–D) are shown with corresponding FACS scatter plots. On the basis of both histology and FACS data, the smallest cell type, spermatids, comprises the largest population in both healthy testes and most TGCTs. As shown in Figure 6F, FACS events consistent with the reported 2 μm size of spermatids comprised 86% of total events in testes tissue, but only 50%, 47%, and 27%, respectively, in the three TGCT samples. Additionally, more diffuse populations, consistent with the

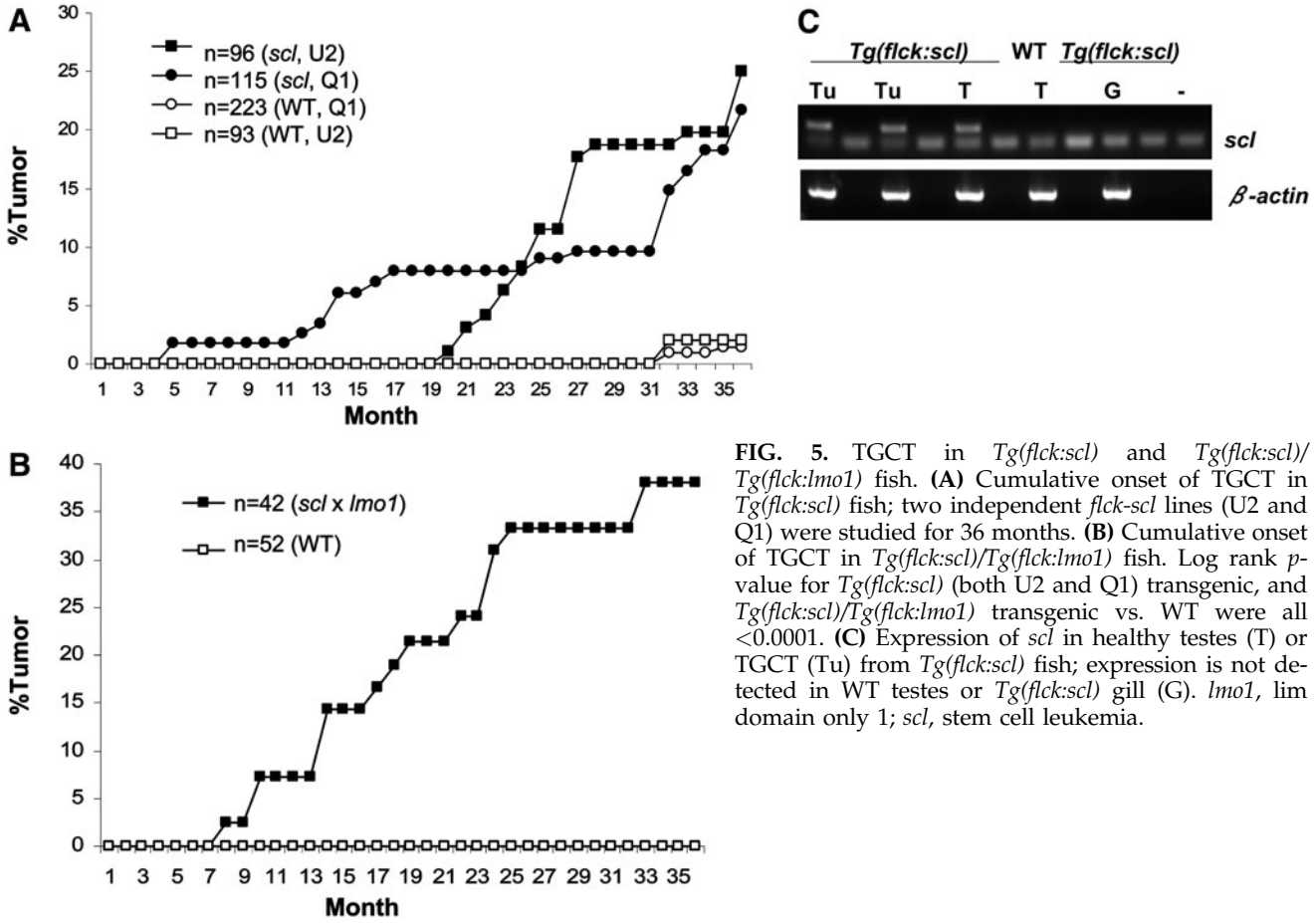

FIG. 5. TGCT in *Tg(flck:scl)* and *Tg(flck:scl)/Tg(flck:lmo1)* fish. **(A)** Cumulative onset of TGCT in *Tg(flck:scl)* fish; two independent *flck-scl* lines (U2 and Q1) were studied for 36 months. **(B)** Cumulative onset of TGCT in *Tg(flck:scl)/Tg(flck:lmo1)* fish. Log rank *p*-value for *Tg(flck:scl)* (both U2 and Q1) transgenic, and *Tg(flck:scl)/Tg(flck:lmo1)* transgenic vs. WT were all <0.0001. **(C)** Expression of *scl* in healthy testes (T) or TGCT (Tu) from *Tg(flck:scl)* fish; expression is not detected in WT testes or *Tg(flck:scl)* gill (G). *lmo1*, lim domain only 1; *scl*, stem cell leukemia.

relatively larger spermatocytes and spermatogonia, ranging in size from 6 to 9 μm in diameter, were increased in all three TGCTs relative to testes.

Discussion

In this report, we describe two zebrafish models for TGCT, using a fugu *lck* promoter to drive expression of *TAg* or *scl* (with or without *lmo1*). Although this study was designed to generate T-cell malignancies, we found that expression of *TAg* or *scl* (with or without *lmo1*) under control of the *flck* promoter led to development of TGCTs in zebrafish. The TGCTs were characterized by obvious abdominal swelling, intra-abdominal organ compression, disorganized testicular architecture, expression of genes associated with human TGCT, and transplantability to healthy WT fish.

The zebrafish is one of the principal vertebrate organisms used to model and study human disease.[28,29] However, to date, there have been few reports describing genetically engineered TGCT in the zebrafish. Previous studies showed that naturally occurring tumors, referred to as gonadal tumors, in male zebrafish can occur between 1 and 2 years of age.[30] These tumors can be up to 10 times as large as healthy testes, asymmetric, multi-lobed, and distinct from other abdominal organs.[31] A recent report described a novel, heritable zebrafish mutant, designated *lamc1*^{cz61}, which showed increased TGCT susceptibility when exposed to carcinogens and chemical mutagenesis.[5] In addition, 17% of *lamc1*^{cz61} fish developed spontaneous TGCTs. However, the mutation responsible for the TGCT predisposition in the *lamc1*^{cz61} fish has not yet been identified.

Several histologically distinguishable types of TGCTs were found in the transgenic zebrafish in our current report. In healthy testes, a typical seminiferous tubule contains a small population of spermatogonia and spermatocytes interspersed with Sertoli cells. During meiosis some of these cells differentiate and migrate toward the lumen. Cells in the inner-most layer of the tubule shed their cytoplasm, and reduce in size to that of a bare nucleus, and are designated spermatids. All of the TGCTs in this study showed a lack of normal organization, with disruption of normal seminiferous tubules. However, in addition to the disruption of normal testicular architecture, a spectrum of additional histologic abnormalities was observed. For instance, Figure 2G shows a TGCT with a homogeneous sheet of spermatocytes, whereas Figure 2F shows a homogeneous sheet of spermatogonial-like cells. In all, tumors comprised of predominantly one cell type accounted for $\sim$10% of all transgenic tumors in this study. The most common type of TGCT in this study was a disorganized accumulation of both spermatocytes and spermatogonial-like cells, as shown in Figure 2E.

Reverse transcription-PCR analysis of *TAg*, *scl*, and *lmo1* demonstrated that these mRNAs were abundantly expressed, under the control of a fugu *lck* promoter, in transgenic zebrafish testes. Although this finding was initially unexpected, since *lck* expression is thought to be restricted to the thymus in

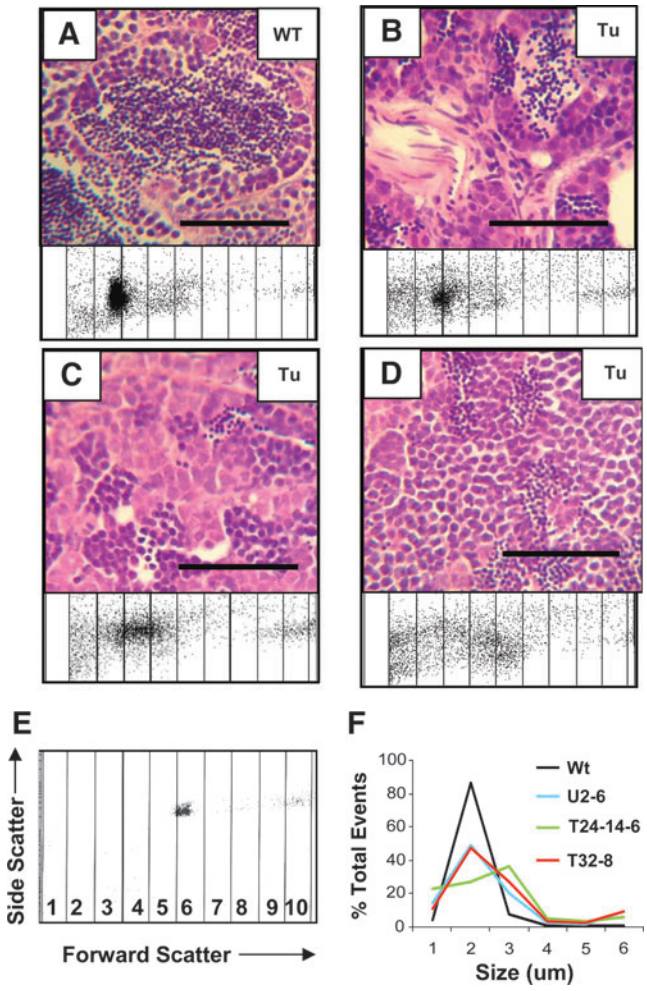

FIG. 6. FACS analysis of TGCT and WT testes. **(A–D)** Hematoxylin and eosin staining compared to FACS forward scatter, divided into 1 μm segments. **(A)** WT testes, **(B)** a TGCT from a *Tg(flck:scl* fish (No. U2-6), **(C)** a TGCT from a *Tg(flck:TAg)* fish (No. T32-8), and **(D)** a TGCT from a *Tg(flck:TAg)* fish (No. T24-14-6). Scale bar is 50 μm. **(E)** Calibration using 6.0–6.4 μm beads. *Y*-axis (side scatter) and *X*-axis (forward scatter) are the same for all FACS plots. **(F)** Percent events versus size as estimated by forward scatter and calibration beads from the TGCT shown in panels **(A–D)**. Note that over 80% of WT events are 2–3 μm in size, consistent with spermatids, whereas the TGCTs have increased numbers of events >3 μm, consistent with spermatocytes and spermatogonia.

mammals, an *EGFP* mRNA driven by this same fugu *lck* promoter was markedly overexpressed in the testes of transgenic mice.[10] Although we have not established the mechanism by which *TAg* is oncogenic in zebrafish testes, by extension of findings in mammalian cells, we speculate that *TAg* acts in zebrafish by complexing p53 and Rb family members. Zebrafish homologs for p53 and p63 have been identified, as have homologs for p107 (RB-like-1), and p130 (RB-like-2), but not pRB (NP_571402.1, NP_694518.1, NP_001124082.1, and XP_001922168.1). Given that *SCL* exerts its leukemogenic effect in mammalian T-cell leukemias by complexing *E2A* and the related *HEB* gene, we suspect that overexpression of zebrafish *scl* leads to a functional depletion of zebrafish *e2a* (*tcf3*) and/or *heb* (*tcf12*) in the zebrafish testes.

Gene expression analysis was carried out on tumors and control testes (Fig. 3), as well as gill, kidney, liver, and intestine tissue. Our goal was twofold: to confirm that the tumor tissue was testicular in origin, and determine whether markers that distinguished TGCT from healthy testes could be identified in the zebrafish. Although expression of all the genes examined could be detected in the TGCTs, expression was also detected in healthy WT and *Tg(flck:TAg)* testes, indicating that none of the genes analyzed could distinguish between healthy testes and TGCTs in this model system.

The survival curves indicated that the TGCTs in transgenic *Tg(flck:TAg)*, *Tg(flck:scl)*, and *Tg(flck:scl)/Tg(flck:lmo1)* zebrafish arose predominantly after 18 months, with an incomplete penetrance. These observations suggest that additional (epi)genetic mutations are required for complete malignant transformation. Given that *KRAS*, *NRAS*, and *HRAS* mutations are frequent in humans with TGCTs, we sequenced *kras*, *nras*, and *hras* from a subset of TGCTs expressing *TAg*; however, we found no mutations in the 10 fish we analyzed, suggesting that *ras* family mutations are not common in the *Tg(flck:TAg)* TGCT model.

In summary, this study reports two transgenic models for TGCTs in zebrafish, produced by ectopic expression of *TAg* or *scl* (as well as a combination of *scl* and *lmo1*) in the testis. The TGCTs were malignant in terms of progressive, inexorable tumor growth, disorganized testicular architecture, effacement of normal testis, and transplantation of the disease to healthy WT fish. These novel models for zebrafish malignancy provide an opportunity to analyze the regulatory mechanisms of zebrafish TGCT development and may lead to new insights regarding the stepwise development of vertebrate testicular tumors.

Acknowledgments

The authors thank Dennis Hickstein, Dave Caudell, and members of the Aplan lab for helpful discussions. The authors thank the Charles River Aquatic staff for excellent animal care.

This research was supported by the Intramural Research Programs of the NCI and NHGRI, NIH.

Disclosure Statement

No competing financial interests exist.

References

1. Ulbright TM. Germ cell neoplasms of the testis. Am J Surg Pathol 1993;11:1075–1091.
2. Skakkebaek NE, Rajpert-De Meyts E, Jorgensen N, Carlsen E, Petersen PM, Giwercman A, *et al.* Germ cell cancer and disorders of spermatogenesis: an environmental connection? APMIS 1998;1:3–11.
3. Shelley MD, Burgon K, Mason MD. Treatment of testicular germ-cell cancer: a cochrane evidence-based systematic review. Cancer Treat Rev 2002;5:237–253.
4. Porcaro AB, Antoniolli SZ, Maffei N, Beltrami P, Bassetto MA, Curti P. Management of testicular seminoma advanced disease. Report on 14 cases and review of the literature. Arch Ital Urol Androl 2002;2:81–85.
5. Neumann JC, Dovey JS, Chandler GL, Carbajal L, Amatruda JF. Identification of a heritable model of testicular germ cell tumor in the zebrafish. Zebrafish 2009;4:319–327.
6. von Hofsten J, Olsson PE. Zebrafish sex determination and differentiation: involvement of FTZ-F1 genes. Reprod Biol Endocrinol 2005;3:63.
7. Orban L, Sreenivasan R, Olsson PE. Long and winding roads: testis differentiation in zebrafish. Mol Cell Endocrinol 2009;312:35–41.
8. Haire RN, Rast JP, Litman RT, Litman GW. Characterization of three isotypes of immunoglobulin light chains and T-cell antigen receptor alpha in zebrafish. Immunogenetics 2000;11:915–923.
9. Chervinsky DS, Zhao XF, Lam DH, Ellsworth M, Gross KW, Aplan PD. Disordered T-cell development and T-cell malignancies in SCL LMO1 double-transgenic mice: parallels with E2A-deficient mice. Mol Cell Biol 1999;7:5025–5035.
10. Pipas JM, Levine AJ. Role of T antigen interactions with p53 in tumorigenesis. Sem Cancer Biol 2001;11:23–30.
11. Brenner S, Venkatesh B, Yap WH, Chou CF, Tay A, Ponniah S, *et al.* Conserved regulation of the lymphocyte-specific expression of lck in the Fugu and mammals. Proc Natl Acad Sci U S A 2002;5:2936–2941.
12. Condorelli GL, Facchiano F, Valtieri FM, Proietti E, Vitelli L, Lulli V, *et al.* T-cell-directed TAL-1 expression induces T-cell malignancies in transgenic mice. Cancer Res 1996;22:5113–5119.
13. Langenau DM, Ferrando AA, Traver D, Kutok JL, Hezel JP, Kanki JP, *et al. In vivo* tracking of T cell development, ablation, and engraftment in transgenic zebrafish. Proc Natl Acad Sci U S A 2004;19:7369–7374.
14. Astrofsky KM, Schrenzel MD, Bullis RA, Smolowitz RM, Fox JG. Diagnosis and management of atypical *Mycobacterium* spp. infections in established laboratory zebrafish (*Brachydanio rerio*) facilities. Comp Med 2000;6:666–672.
15. Watral V, Kent ML. Pathogenesis of *Mycobacterium* spp. in zebrafish (*Danio rerio*) from research facilities. Comp Biochem Physiol C Toxicol Pharmacol 2007;1:55–60.
16. Wang XG, Orban L. Anti-mullerian hormone and 11 beta-hydroxylase show reciprocal expression to that of aromatase in the transforming gonad of zebrafish males. Dev Dyn 2007;5:1329–1338.
17. Sakai N. *In vitro* male germ cell cultures of zebrafish. Methods 2006;39:239–245.
18. Yano A, Suzuki K, Yoshizaki G. Flow-cytometric isolation of testicular germ cells from rainbow trout (*Oncorhynchus mykiss*) carrying the green fluorescent protein gene driven by trout vasa regulatory regions. Biol Reprod 2008;1:151–158.
19. Egydio de Carvalho C, Tanaka H, Iguchi N, Ventela S, Nojima H, Nishimune Y. Molecular cloning and characterization of a complementary DNA encoding sperm tail protein SHIPPO 1. Biol Reprod 2002;3:785–795.
20. de Waal PP, Leal MC, Garcia-Lopez A, Liarte S, de Jonge H, Hinfray N, *et al.* Oestrogen-induced androgen insufficiency results in reduction of proliferation and differentiation of spermatogonia in the zebrafish testis. J Endocrinol 2009;2:287–297.
21. Almstrup K, Hoei-Hansen CE, Nielsen JE, Wirkner U, Ansorge W, Skakkebaek NE, *et al.* Genome-wide gene expression profiling of testicular carcinoma *in situ* progression into overt tumours. Br J Cancer 2005;10:1934–1941.
22. Gashaw I, Dushaj O, Behr R, Biermann K, Brehm R, H. Rubben H, *et al.* Novel germ cell markers characterize testicular seminoma and fetal testis. Mol Hum Reprod 2007;10:721–727.
23. Pauls K, Jager R, Weber S, Wardelmann E, Koch A, Buttner R, *et al.* Transcription factor AP-2gamma, a novel marker of gonocytes and seminomatous germ cell tumors. Int J Cancer 2005;3:470–477.
24. Mulder MP, Keijzer W, Verkerk A, Boot AJ, Prins ME, Splinter TA, *et al.* Activated ras genes in human seminoma: evidence for tumor heterogeneity. Oncogene 1989;11:1345–1351.
25. Amsterdam A, Lai K, Komisarczuk AZ, Becker TS, Bronson RT, Hopkins N, *et al.* Zebrafish Hagoromo mutants upregulate fgf8 postembryonically and develop neuroblastoma. Mol Cancer Res 2009;7:841–850.
26. Youngren KK, Coveney D, Peng X, Bhattacharya C, Schmidt LS, Nickerson ML, *et al.* The Ter mutation in the dead end gene causes germ cell loss and testicular germ cell tumours. Nature 2005;7040:360–364.
27. Moore JL, Rush LM, Breneman C, Mohideen MA, Cheng KC. Zebrafish genomic instability mutants and cancer susceptibility. Genetics 2006;2:585–600.
28. Kawakami K. Transposon tools and methods in zebrafish. Dev Dyn 2005;2:244–254.
29. Allen JP, Neely MN. Trolling for the ideal model host: zebrafish take the bait. Future Microbiol 2010;4:563–569.
30. Smolowitz R, Hanley J, Richmond H. A three-year retrospective study of abdominal tumors in zebrafish maintained in an aquatic laboratory animal facility. Biol Bull 2002;2:265–266.
31. Spitsbergen JM, Tsai HW, Reddy A, Miller T, Arbogast D, Hendricks JD, *et al.* Neoplasia in zebrafish (*Danio rerio*) treated with N-methyl-N′-nitro-N-nitrosoguanidine by three exposure routes at different developmental stages. Toxicol Pathol 2000;5:716–725.

Address correspondence to:
Peter D. Aplan, M.D.
Genetics Branch, Center for Cancer Research
National Cancer Institute, NIH
Navy 8, Room 5101
8901 Wisconsin Ave.
Bethesda, MD 20889

E-mail: aplanp@mail.nih.gov